

Novel isoforms of the β and γ subunits of the *Xenopus* epithelial Na channel provide information about the amiloride binding site and extracellular sodium sensing

(aldosterone/sodium transport/sodium self-inhibition)

ALESSANDRO PUOTI*[†], ANNE MAY*, BERNARD C. ROSSIER, AND JEAN-DANIEL HORISBERGER[‡]

Institut de Pharmacologie et de Toxicologie, Rue du Bugnon 27, CH-1005 Lausanne, Switzerland

Communicated by Robert W. Berliner, Yale University School of Medicine, New Haven, CT, March 17, 1997 (received for review January 6, 1997)

ABSTRACT We have previously identified three homologous subunits α , β , and γ of the highly selective amiloride-sensitive Na channel from the *Xenopus laevis* kidney A6 cell line, which forms a tight epithelium in culture. We report here two novel genes, termed $\beta 2$ and $\gamma 2$, which share 90 and 92% sequence identity with the previously characterized β and γ XENaC, respectively. $\beta 2$ and $\gamma 2$ transcripts were detected in lung, kidney, and A6 cells grown on porous substrate. The physiological and pharmacological profile of the Na channel expressed after $\alpha\beta 2\gamma$ XENaC cRNA injection in *Xenopus* oocyte did not differ from $\alpha\beta\gamma$ XENaC. By contrast, the channel expressed after $\alpha\beta\gamma 2$ injection showed: (i) a lower maximal amiloride-sensitive sodium current, (ii) a higher apparent affinity for external sodium and inactivation of the sodium current by high sodium concentrations, and (iii) a lower apparent affinity for amiloride (K_i $\alpha\beta\gamma 2$; 1.34 μM versus $\alpha\beta\gamma$ 0.35 μM). These data indicate that the γ (and/or $\gamma 2$) subunit participates in amiloride binding and the sensing of the extracellular sodium concentration. The close homology between γ and $\gamma 2$ will help to define the domains involved in sensing external sodium and in the structure of this important drug receptor.

In tight epithelia, electrogenic sodium reabsorption is mediated by a sodium-selective amiloride-sensitive channel, located in the apical membrane facing the external compartment (1–3). This channel is the rate limiting step in sodium reabsorption and control of its activity is essential to the maintenance of the global sodium balance and blood pressure (4). The biophysical properties of the highly selective epithelial Na channel have been well defined in the apical membrane of the rat cortical collecting duct (5) and that of the A6 cell line (6), a cell line derived from the *Xenopus laevis* kidney. In both A6 cells and rat cortical collecting duct the highly selective Na channel is characterized by: (i) its high sodium selectivity with a $P_{\text{Na}}/P_{\text{K}}$ as high as 30, (ii) a low single-channel conductance (4–5 pS), (iii) a gating kinetics characterized by long times of closures and openings (in the range of a few seconds), and (iv) a high sensitivity to amiloride (K_i in the submicromolar range) (3). There are other types of sodium-permeable channels in epithelial cells and they can be classified according to their amiloride sensitivity or to their ion selectivity (3, 7). According to Palmer's classification (3), in addition to the highly selective 5 pS (Type 1) Na channel, there is a 9 pS (Type 2) channel with a lower ionic selectivity ($P_{\text{Na}}/P_{\text{K}}$ around 4) and a nonselective cation channel (Type 3). We have recently identified the primary structure of a Type 1 ENaC of the rat distal colon epithelium (8, 9). We proposed that the rat epithelial Na channel is a heterooligomeric protein, made of three homologous subunits, the α , the β , and the

γ rENaC. The cloning of the α , β , and γ subunits from human tissues has also been recently reported (10–13).

We have also identified three homologous subunits (α , β , and γ XENaC) from the cell line A6 (14). Besides the 2.4-kb β transcript, Northern blot analysis of lung and kidney revealed additional bands of higher molecular weight, suggesting the presence of other gene products. We report here two novel genes, termed $\beta 2$ and $\gamma 2$, which share 90 and 92% sequence identity with the previously characterized β and γ XENaC, respectively, and the initial physiological characterization of the channel formed using these subunits.

MATERIALS AND METHODS

Cells and Cell Culture Procedures. A6 cells (passage 80–90), from the American Type Culture Collection, were re-cloned by limiting dilution and grown on plastic dishes at a density of $1.2 \times 10^6/\text{cm}^2$. The subclone used in this study (A6–2F3) has been previously described (15). For experiments with cells grown on plastic substrate, A6 cells were cultured until they formed a confluent monolayer and stimulated with aldosterone or control-incubated. Unstimulated cells were used to seed semipermeable filters (Costar 3419) on which cells were allowed to grow for 10 more days, before aldosterone stimulation and extraction.

Isolation of Poly(A)⁺ RNA. Total RNA was isolated from A6 cells grown on a plastic substrate or permeable filters. In some instances cells were previously stimulated for 24 hr with 300 nM of aldosterone (Sigma). Cells were lysed in 0.5% SDS, 100 mM NaCl, 1 mM EDTA, 20 mM Tris-HCl (pH 7.5) and digested with proteinase K (200 $\mu\text{g}/\text{ml}$, Sigma) for 1 hr at 37°C. poly(A)⁺ RNA was purified by oligo(dT) cellulose-affinity chromatography (16). Typical yields were 110 μg of poly(A)⁺ from 24 filters or 30 Petri dishes. poly(A)⁺ RNA from A6 cells destined to cDNA libraries was further enriched in channel activity by size fractionation on a 5–20% sucrose gradient and functional activity test in oocytes (14, 17). poly(A)⁺ RNA from fresh tissues of *Xenopus* was extracted as mentioned above except that the RNAs were not enriched on sucrose gradients. poly(A)⁺ RNA from *Xenopus* oocytes was extracted as follows: 200 oocytes, selected for stage, were lysed by Polytron in 10 mM Tris-HCl (pH 7), 1.5 mM MgCl₂, 10 mM NaCl, 2% SDS, 0.3 M sodium acetate (pH 5.2), 2 $\mu\text{g}/\text{ml}$ proteinase K and incubated at 37°C for 1 hr. The lysate was extracted several times with phenol chloroform and nucleic acids were precipitated overnight with 2.5 vol of absolute ethanol at –20°C. poly(A)⁺ was purified using oligo(dT) resin.

Abbreviation: RT, reverse transcriptase.

Data deposition: The sequences reported in this paper have been deposited in the GenBank database (accession no. Y12000 for β and Y12001 for $\gamma 2$). *A.P. and A.M. contributed equally to this study and may be cited in either order.

[†]Present address: Howard Hughes Medical Institute and Department of Biochemistry, 420 Henry Mall, Madison, WI 53706.

[‡]To whom reprint requests should be addressed.

The publication costs of this article were defrayed in part by page charge payment. This article must therefore be hereby marked "advertisement" in accordance with 18 U.S.C. §1734 solely to indicate this fact.

Copyright © 1997 by THE NATIONAL ACADEMY OF SCIENCES OF THE USA
0027-8424/97/945949-6\$2.00/0
PNAS is available online at <http://www.pnas.org>.

Identification of $\beta 2$ and $\gamma 2$ XENaC. First-strand cDNA synthesis was performed on 2–3 μg of poly(A)⁺ RNA using superscript reverse transcriptase (RT) (Superscript II, BRL), 500 μM of dNTPs and oligo(dT) (Pharmacia, 0.1 $\mu\text{g}/\mu\text{l}$). Fragments of $\beta 2$ or $\gamma 2$ XENaC were amplified using *Taq* DNA polymerase (Boehringer Mannheim) and degenerated oligonucleotides designed to recognize nonselectively all potential α , β , and γ subunits of XENaC (14). The sense 5' primer was: 5'-GGIAA(C/T)TG(C/T)TA(C/T)ACITT(C/T)AA-3', corresponding to the amino acids GNCYTFN (positions [AA] 262–268 in α XENaC). The antisense 3' primer was:

5'-CGCGGATCCCAT(A/G)TT(C/T)TC(C/T)TG(A/G)AA(A/G)CA-3'. It corresponds to the sequence CFQENM (positions [AA] 381–386 in α XENaC) and contains a *Bam*HI site on its 5' end.

PCR reactions were performed in *Taq* DNA polymerase buffer (Boehringer Mannheim) supplemented with 80 μM of dNTP, 250 ng of the 5' and the 3' degenerate sense and antisense oligonucleotides, 10–30 ng of single-stranded cDNA, and 1 unit of *Taq* DNA polymerase. Cycles were as follows: addition of the enzyme at 94°C, followed by 30 cycles of 1 min at 94°C, 2 min at 42°C, and 1.5 min at 72°C. PCR products of expected size (390 nt) were purified and blunted using T4 DNA polymerase (5 min at 16°C) and phosphorylated with polynucleotide kinase (New England Biolabs). The fragments were digested with *Bam*HI, purified on an agarose gel, and subcloned into pBluescript KS(II) (Stratagene) and sequenced.

Once one subunit was identified it was removed from the reaction mixture by digestion with restriction endonucleases, which were specific for a given subunit (for instance *Sty*I for α XENaC, *Xba*I for β XENaC, *Nco*I for γ XENaC, *Pvu*II for $\beta 2$ XENaC, and *Bcl*I for $\gamma 2$ XENaC). Undigested material was purified on an agarose gel and an aliquot was used to reinitiate a second PCR reaction under the same experimental conditions. Amplified products were subjected to a second/third round of digestion with the same restriction endonuclease and only the resistant material was subcloned and sequenced.

Isolation of Full-Length Clones. Two plasmid cDNA libraries were constructed; one from A6 cells grown on filters and one from *Xenopus* kidney, using standard procedures (SuperScript Plasmid System, BRL). The 5' *Sal*I-adapted cDNA was digested with *Not*I and cloned into the pSPORT vector (BRL). For the $\gamma 2$ XENaC screen, a cDNA library of 300,000 independent clones from aldosterone-stimulated A6 cells cultured on filters was divided into 26 pools and first screened by PCR using specific oligonucleotides for $\gamma 2$ XENaC. For $\beta 2$ XENaC, a cDNA library from *Xenopus* kidney (150,000 independent clones) also divided into pools was screened with specific oligonucleotides. Positive pools ($\approx 12,000$ clones) were then screened with the corresponding PCR-generated DNA fragments. A specific probe for $\beta 2$ XENaC was available, whereas the $\gamma 2$ XENaC probe also recognized γ XENaC. $\gamma 2$ XENaC clones were distinguished from γ XENaC by PCR. All polynucleotide probes were labeled with [α -³²P]dCTP using standard procedures (Random-Primed Labeling kit, Boehringer Mannheim). The hybridization conditions were 20% of formamide, 5 \times SSC, 2 \times Denhardt's solution, 0.1% SDS, and 150 $\mu\text{g}/\text{ml}$ of denatured salmon sperm DNA at 42°C. Nylon membranes (Hybond-N, Amersham) were washed in 1 \times SSC at 42–50°C and exposed at –70°C. Full-length clones were analyzed by sequencing using the chain-termination reaction and T7 DNA polymerase (United States Biochemicals).

Northern Blot Analysis and RT-PCR. poly(A)⁺ RNA isolated from fresh organs of *X. laevis* or cultured A6 kidney cells was electrophoresed on a 1% denaturing glyoxal agarose gel and blotted to Hybond-N membranes and cross-linked. The membranes were hybridized with 390-nt long PCR-generated probes specific to either α , β , or γ XENaC (14). The probes for β XENaC and γ XENaC recognized both β and $\beta 2$ XENaC and γ and $\gamma 2$ XENaC, respectively. A 350-nt probe specific to $\beta 2$ XENaC was obtained by PCR from the 3' untranslated region of $\beta 2$ XENaC.

Hybridization conditions were for 16 hr at 42°C in 25% formamide, 5 \times SSC, 5 \times Denhardt's solution, 0.1% SDS, and 150 $\mu\text{g}/\text{ml}$ of denatured salmon sperm DNA. Blots were washed at 42–50°C in 1 \times SSC and exposed for 1–5 days at –70°C.

The presence of $\beta 2$ and $\gamma 2$ XENaC transcripts was also checked by PCR in kidney, lung, and A6 cells grown under different conditions. Oligonucleotides specific to each of the identified subunits were used, and negative controls were included in all PCR runs.

$\gamma/\gamma 2$ Chimeric Constructs. Two pairs of symmetric chimeric peptide composed of part of the γ and part of the $\gamma 2$ were constructed. A first chimera (N1-c2) was composed of a large γ N-terminal segment comprising the N-terminal cytoplasmic domain, the first hydrophobic segment and most of the extracellular loop, and of the second hydrophobic segment and the C terminus of $\gamma 2$ (cutting point at amino acid position 460, *Pst*I site). The second chimera (N2-c1) was the symmetric construct. In the third and fourth constructs (n1-C2 and n2-C1), the cutting point was located at amino acid position 171 (*Pvu*II site) in the initial part of the extracellular loop (see scheme in Fig. 7). These chimeric constructs were subcloned into the *Sal*I–*Not*I sites of the pSPORT1 expression vector.

Functional Expression in *Xenopus* Oocytes. To improve and to standardize cRNA synthesis rate, all ENaC subunits were recloned as *Sal*I–*Not*I fragments into a modified pSD5 vector, containing a part of the polylinker of the Bluescript vector and 100 adenosine residues downstream to the insert. SP6 RNA polymerase (Promega) was used for cRNA synthesis. Typically, 1 ng of cRNA subunit per oocyte was injected in a total volume of 50 nl. The amiloride-sensitive sodium current was measured after 2–3 days of incubation.

Measurement of amiloride-sensitive current in oocytes. Using the two-electrode voltage-clamp technique, amiloride-sensitive currents were measured as described (9) at room temperature (22–25°C) and at –100 mV in a solution containing 100 mM sodium gluconate, 2 mM KCl, 1.8 mM CaCl₂, 10 mM Hepes (pH 7.2), 5 mM BaCl₂, and 10 mM tetraethylammonium chloride.

Apparent affinity for amiloride. The inhibition constant (K_I) for amiloride was obtained by measuring the whole cell current after successive addition of five concentrations of amiloride ranging from 50 nM to 50 μM . Affinity values were obtained by fitting the parameters of a single-site binding equation to the current inhibited by amiloride (I_{am})

$$I_{am} = I_{am,max}/(1 - K_I/[am]),$$

where $I_{am,max}$ is the maximal current inhibition and [am] the concentration of amiloride.

Apparent affinity for Na⁺. The apparent affinity of ENaC for Na⁺ was measured as the half activation constant ($K_{1/2Na}$) of the amiloride-sensitive current. Amiloride-sensitive currents were measured in solutions containing 0, 1, 3, 10, 30, or 100 mM Na⁺, obtained by equimolar replacement of Na⁺ gluconate by *N*-methyl-D-glucamine (NMDG) gluconate. A high concentration of amiloride (50 μM) was used for these experiments to ensure an equally complete inhibition of the current through the ENaC isoforms. In the absence of external Na⁺, outward amiloride-sensitive currents were observed even at –100 mV. These currents were of small but variable amplitude, probably depending on the state of sodium loading of the oocytes. To obtain a correct relationship between external sodium concentration and inward sodium current, the outward amiloride-sensitive currents measured in the absence of external Na⁺ were subtracted from the currents measured at each sodium concentration.

RESULTS

Primary Structure of the $\beta 2$ and $\gamma 2$ Subunits of XENaC. We identified two new genes products of *X. laevis* coding for proteins that belong to the epithelial Na channel family. The two clones have been termed $\beta 2$ and $\gamma 2$ because of the high

degree of homology with the formerly known XENaC β and γ subunit, respectively. The β_2 clone is 2686 nt long and contains a single open reading frame encoding a 646 amino acid peptide. The γ_2 clone is 3665 nt long with a single open reading frame encoding a 662 residue peptide. The degree of similarity is generally high, but significantly lower in the noncoding region than in the coding region. The nucleotide sequence identity amounts to 92.3% between β and β_2 isoforms and 90.6% between γ and γ_2 in the coding region. It averages about 58% between β and β_2 isoforms and about 56% between γ and γ_2 in the available parts of the 3' and 5' noncoding regions.

The amino acid sequences deduced from the β_2 and γ_2 clones are shown in Fig. 1, aligned with the known β and γ subunit peptides. The similarity between β and β_2 isoforms at the protein level is very high, with only 45 different residues and 1 single amino acid deletion (= 93.0% identity, β_2 versus β). The similarity is slightly lower between the γ and γ_2 peptides with 58 different residues and an addition of 3 residues (= 91.2% identity, γ_2 versus γ).

Tissue Distribution. Northern blot analysis (Fig. 2) showed that the β_2 isoform could be observed as a 2.9-kb transcript in kidney at a relatively high level, similar to the level of the β isoform in this organ. It was present with a lower abundance in lung, where a clear dominance of the β isoform was present. A weak β_2 signal was also detected in A6 cells grown on permeable support, but not in A6 cells grown on plastic. The 3.8-kb γ_2 transcript was relatively abundant in A6 cells grown on permeable support, although at a much lower level than the γ isoform. It could never be detected in A6 cells grown on plastic and was not detected by Northern blot analysis in kidney or lung (Fig. 2D). When probed with α XENaC, one single 3.0-kb transcript was detected in all tested tissues.

These results were generally confirmed by RT-PCR of the same transcript (Fig. 3). Fragments with the expected size for the β_2 transcript were detected in kidney, lung, and A6 cells grown on filters, but not in A6 cells grown on plastic. The β_2 and γ_2 signals were most evident in A6 cells grown on filter, detectable in lung and kidney, but always absent in A6 cells grown on plastic.

Functional Expression of β_2 and γ_2 Subunits of XENaC in *Xenopus* Oocytes.

Expression and affinity for amiloride. To compare the functional characteristics of the new isoforms of the β and γ subunits we studied the amiloride-sensitive current in oocytes injected with

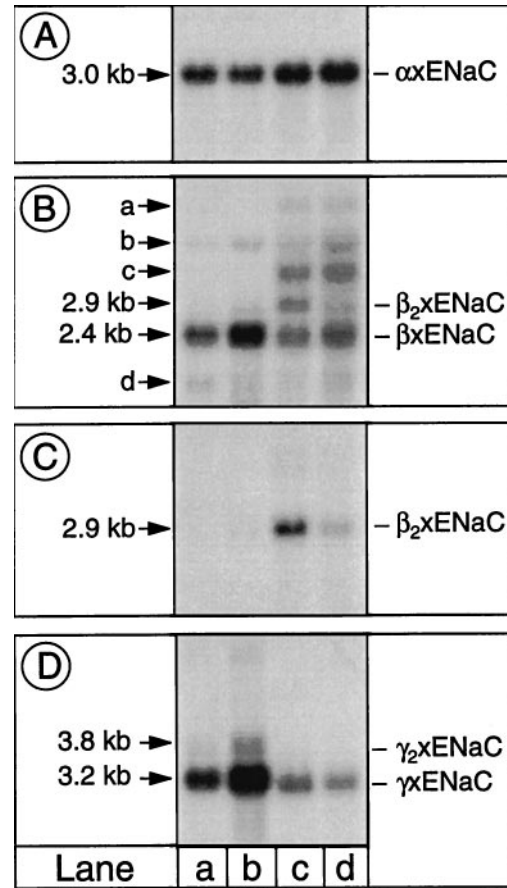


FIG. 2. Tissue distribution by Northern blot analysis. Northern blot analysis of α , β , β_2 , γ , and γ_2 transcript in lung, kidney, and A6 cells grown either on plastic or on permeable support. poly(A)⁺ RNA (3 μ g) were loaded in lanes a (A6 cells grown on plastic) and b (A6 cells grown on filters), whereas 5 μ g of poly(A)⁺ RNA was loaded in lanes c (kidney) and d (lung). The probes used to recognize α (A), β (B), β_2 (C), and γ (D) have been described. The probe for β XENaC (B) also recognizes β_2 XENaC and four other transcripts, but their presence was not consistent from one RNA extraction to another. (C) The same blot was probed with a fragment, which specifically recognized β_2 XENaC.

β_2	MIQGLKRLK	RYFTRALHRI	QKGPYTYKE	LLVWFCDNTN	THGPKRI-IK	EGPKKRVWVF	ILTLVFAGLV	FWQWGLLILT	YLSYGVSVSL	SIGFKTMEFP	99
β	H.M							V			99
β_2	AVTVCNPNPY	KYSRVKPLK	DDELVATAL	DRIQYSSQIQ	ANTFTYNN-T	RQNVTLDPAL	WNHIPLVVID	ENDPCNPVIH	NI-FDMSVFI	SKNNLLRNSS	197
β	L.A.F	E		F.N	G.H.Q			T.R.I	NAV	SSI	198
β_2	EDQTSYAQR	KVAMKLC-TN	NMTQCVRNF	TSGVQALREW	YLLQLSIFIS	NVPLSDRVDM	GFKAE DLILT	CLFGGQPCSY	RNFTHIYDAD	YGNCYIFNWS	296
β											297
β_2	QEGDDTMSSA	NPADPGLKL	VLDIEQDEYL	PFLQTTAAAR	LILHQQRFP	FVKDLGIYAK	PGTETSIAVL	VDLQOQMEAP	YSSCTVNGSD	IPVQNLVEEF	396
β	EN		G					EH			397
β_2	NSSYSIQSCL	RSCYQEEMVK	TCKCAHYQYP	LPNGSEYCTN	NKHPDWVPCY	YSL-RDSVAI	RENCISLCQQ	PCNDTHYKMV	ISMADWPSAG	AEDWIFHVLS	495
β					M						496
β_2	YEKSSYDIT	VNRNGIVRLN	IYQEFNYRS	ISESEATNVV	WLLSNLGGQF	GFWMGGSVLC	IIEFGEI-II	DCMWITILKL	LAWIRNRRQR	RQRQYADPP	594
β	HN								R	K.S	595
β_2	PTVSELVEAH	TNP-----	GFQHDGDNHV	TED-----	---IPGTPPP	NYDSLVRNTI	---EPVSSDE	EN	646		
β		S-----	Q.H.D.D	PV-----	---	Y.S	---		647		
γ_2	MSNSGKLLT	QKLKKNL-PV	TGPQAPTLYE	LMQWYCLNTN	THGCRRIVVS	KGLRRLRVIWI	VLTLIAVALI	FWQCALLMST	Y--YSVSASI	TVTFQRLVYP	96
γ	K						S.C.V	S			96
γ_2	AVTICNPNPY	YSYKIKDRLA	TLEKTTNQT	KNI-YGFTEP	LIRSKRDLV	NDENSTEDIF	LKQIPLFRLE	SIKGNQLVVS	DLKTKKRTQI	SGKVIQRDAG	195
γ		V	A.E.S		V.G	V	Y	V.S	RM	A.H.E	195
γ_2	SVQDS---DN	MVGFKLCDAN	NSSDCTIFTF	GSVNAIQEW	YRLHYNLILA	KISMEDKIAM	GKADELIVT	CLFDGLSCDA	RNFTLFHHP	YGNCYTFNSA	292
γ	P---G	PK	S		T			F			292
γ_2	ERG-NLLVSS	MGAEYGLKV	VLYIDEDEYN	PYLSTAAGAK	LLVHDQDEYP	FIEDLGTLE	TGTETSIGMQ	LTESTKLSDF	YSDCTIDGSD	LSVENLY---	388
γ									A.M.R	V	388
γ_2	NKKYTLQICL	NSCFQREMVR	SCGCAHYDQP	LPNGAKYCNV	EEYPNWIYCY	VKLYKQFVQE	ELGCQSTCRE	SCSFKEWTLT	RSLAKWPSLN	SEEWMLRVLVS	487
γ					S	F.V	A				488
γ_2	WELGEKLNKN	LTKNDLGNLN	IFYQDLNRS	ISESPTYNIV	TLLSNFSGQL	GLWMSCSMIC	VLEIIEVFFI	DSFWVILRQK	WHKLCNWNKN	RKENIEEIP	587
γ		A						V.R	R	E	588
γ_2	DIIVPAMAGH	NNPLCVDHPI	CLGEDDPPTF	HSAQLPQAQ	DCRVPRTPPP	KYNTLRIQSA	FQLETIDSDE	DVERF	662		
γ	E.P.T.T	D	E	N	S	SH		L	660		

FIG. 1. Sequence of the novel β_2 and γ_2 subunit of XENaC. The deduced amino acid sequences of the β_2 and γ_2 isoforms are aligned with the corresponding β and γ XENaC subunits [output of the pileup program of the Genetics Computer Group sequence analysis software package (18)]. Dots indicate that the residue in the β isoform is identical to the same position in the β_2 isoform, and similarly for the γ and γ_2 subunits. A dash indicates that a gap was introduced for obtaining a best-fit alignment. Lines above sequences indicate the positions of the putative transmembrane segments.

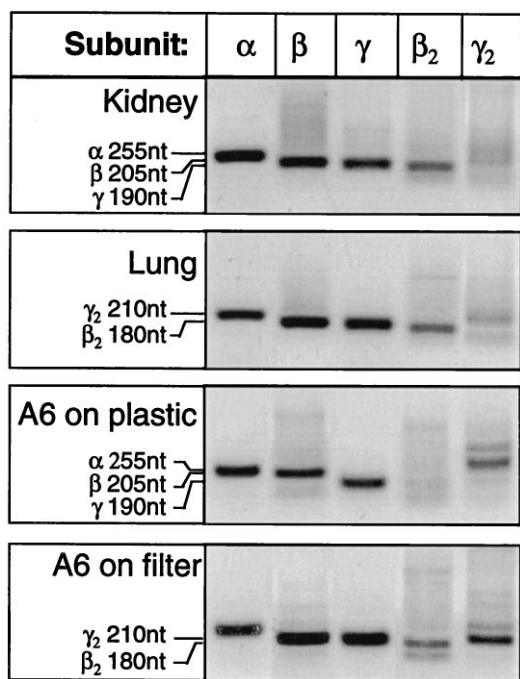


FIG. 3. Tissue distribution by RT-PCR. RT-PCR analysis in the same tissues. The transcripts of all five subunits were present in kidney, lung, and A6 cells grown on a porous substrate. Transcripts of the expected size for β_2 and γ_2 XENaC could never be detected when single-stranded cDNA derived from RNA from A6 cells grown on plastic was used as a template. Considering the high sensitivity of the RT-PCR methods, this makes unlikely the presence of a significant number of these transcripts in cells grown on plastic.

the following combinations of subunit cRNA: $\alpha\beta\gamma$, $\alpha\beta_2\gamma$, $\alpha\beta\gamma_2$, and $\alpha\beta_2\gamma_2$. Fig. 4 shows the results of the current sensitive to 20 μM of amiloride (a) and the apparent affinity for amiloride of

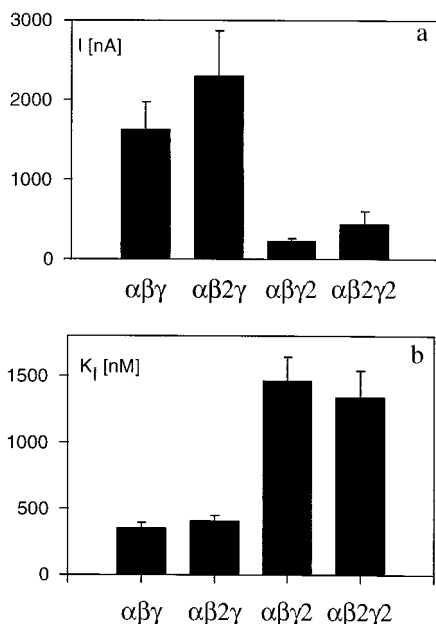


FIG. 4. Amiloride-sensitive current in isoforms of XENaC. Oocytes injected with the indicated combination of cRNA α , β , and γ subunits were studied under voltage-clamp conditions at -100 mV in a 100 mM sodium amphibian Ringer. (a) The current inhibited by a high concentration of amiloride (20 or 50 μM). The number of observations were 41, 25, 23, and 18 for the $\alpha\beta\gamma$, $\alpha\beta_2\gamma$, $\alpha\beta\gamma_2$, and $\alpha\beta_2\gamma_2$ groups, respectively. (b) The inhibitory constant of amiloride in each group. The number of measurements were 10, 4, 7, and 8 in $\alpha\beta\gamma$, $\alpha\beta_2\gamma$, $\alpha\beta\gamma_2$, and $\alpha\beta_2\gamma_2$, respectively.

these ENaC isoforms (b). The amplitude of the amiloride-sensitive current was reduced in the heteromer including the γ_2 isoform compared with those including the γ isoform. The oocytes expressing $\alpha\beta\gamma_2$ had, however, a much larger amiloride-sensitive current than the oocyte expressing $\alpha\beta$ without any γ subunit, in which the amiloride-sensitive current was often not detectable (4.8 ± 1.2 nA, $n = 20$). The γ_2 isoform also conferred a significantly lower affinity for amiloride by a factor of about 3. In contrast, no significant difference of level of expression or of affinity for amiloride could be observed between heteromers expressing the β and β_2 isoform.

Relationship between the amiloride-sensitive sodium current and the sodium concentration. Because of the functional difference between ENaC isoforms including the γ and γ_2 subunits with regards to amiloride binding, we also examined the effect of the type of γ subunit on the affinity for Na^+ . The relationship between external Na^+ concentration and amiloride-sensitive inward current at -100 mV is shown in Fig. 5. It should be noted that Fig. 5 shows current as values relative to those measured with 100 mM Na^+ ; the absolute values were in fact about 10 larger in the $\alpha\beta\gamma$ group than in the $\alpha\beta\gamma_2$ group (for exact values see the legend of Fig. 5). In the oocytes expressing the $\alpha\beta\gamma$ isoform the relationship was reasonably well described by a simple one-site activation kinetic with a $K_{1/2}$ of about 10 mM. In the $\alpha\beta\gamma_2$ group the relationship was clearly different. First, I_{am} was consistently smaller in the presence of 100 mM Na^+ than in 30 mM Na^+ . Second, the concentration needed to activate a current with an amplitude of one-half of the maximal amplitude was about 2.8 mM (although no meaningful $K_{1/2}$ value could be obtained because of the poor quality of the fit with a one-site activation kinetic equation). In Fig. 5, the current/concentration relationship of the $\alpha\beta\gamma_2$ group is shown with a fit to a two-site equation (see Fig. 5 legend) with one high-affinity activating site ($K_{1/2}$ 4.9 \pm 0.14) and one low-affinity inhibitory site ($K_{1/2}$ 154 \pm 6 mM). The reasons for using this equation were first, the need for a biphasic effect of sodium concentration and second, the experimental evidence for a $\text{Na} \ll \text{self-inhibition} \gg$ site (1).

Na^+ /amiloride interaction. The binding of amiloride to the Na channel of tight epithelia is known to be inhibited by external Na^+ in a competitive manner (1). To investigate the relation-

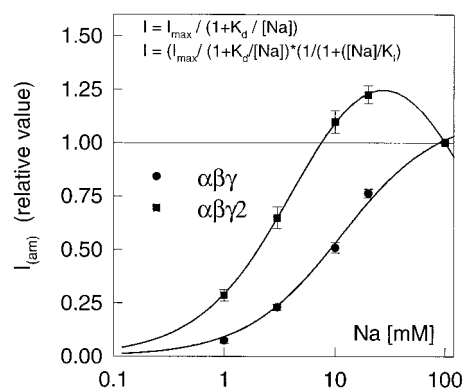


FIG. 5. Kinetics of the activation by sodium of the amiloride-sensitive current. The current sensitive to 50 μM amiloride at -100 mV, I_{am} , was measured in solutions containing 0, 1, 3, 10, 20, and 100 mM Na^+ . All current values were normalized to the value of the amiloride-sensitive current in 100 mM Na, which was $3,630 \pm 1,070$ nA ($n = 12$) in the $\alpha\beta\gamma$ group and 167 ± 73 nA ($n = 8$) in the $\alpha\beta\gamma_2$ group. In the $\alpha\beta\gamma$ group the sodium concentration/ I_{am} relationship was well described by simple Michaelis-Menten kinetics (upper equation) with a K_d of 11.3 mM. In the $\alpha\beta\gamma_2$ group the sodium concentration/ I_{am} relationship was obviously different, with a significantly lower value in 100 mM Na^+ than in 20 mM Na^+ . The curve fitted to the $\alpha\beta\gamma_2$ data points (lower equation) represents a double effect of Na^+ concentration on the amiloride-sensitive current; first, an activation effect with a K_d of 4.8 mM and second, an inhibitory effect with a K_i of 154 mM.

ship between the effect of the γ and γ_2 isoforms on the affinity for amiloride and sodium, we measured the amiloride half-inhibition constant (K_i) in solution containing 2.5, 10, 25, or 100 mM Na^+ (solutions prepared by NMDG replacement as described). The results of these measurements are summarized in Fig. 6. Assuming competitive binding to a single site, the apparent affinity for amiloride should decrease with increasing concentration of external Na^+ , according to

$$K_{i\text{app}} = K_i(1 + [\text{Na}]/K_{d\text{Na}}), \quad [1]$$

where $K_{i\text{app}}$ is the apparent K_i for a given Na^+ concentration, $[\text{Na}]$ is the external Na^+ concentration, and $K_{d\text{Na}}$ the affinity of Na^+ for the amiloride binding site. Eq.1 can also be written as

$$K_{i\text{app}} = K_i + [\text{Na}](K_i/K_{d\text{Na}}), \quad [2]$$

where $K_{i\text{app}}$ appears as a linear function of $[\text{Na}]$. Fig. 5 shows that in both group there was a linear relationship between the apparent K_i and the Na^+ concentration. The intercept of the regression line yielded values very close to 160 nM for both groups, indicating that the intrinsic affinity (i.e., the affinity in the absence of competing Na^+ ions) of amiloride for its binding site was similar in both groups. From the slope of the regression lines of the $K_{i\text{app}}$ versus $[\text{Na}]$ plot an affinity of Na^+ for the amiloride site could be calculated: it was 55 mM for the $\alpha\beta\gamma$ isoform and 12 mM for the $\alpha\beta\gamma_2$ isoform.

We then measured the amiloride affinity in oocyte injected with α and β subunits cRNA and with either γ or γ_2 or one of four γ/γ_2 chimeric constructs as described in Fig. 7. The chimera in which the transition point was located shortly after the first hydrophobic region (**n1-C2**: N-terminal γ /C-terminal γ_2 , or **n2-C1**: N-terminal γ_2 /C-terminal γ) yielded amiloride K_i values intermediate between those obtained with wild-type γ and γ_2 , but with the chimeras in which the transition point was located close to the end of the extracellular loop region (**N1-c2**: N-terminal γ /C-terminal γ_2 , or **N2-c1**: N-terminal γ_2 /C-terminal γ), a low affinity was clearly associated with the γ_2 N-terminal two-thirds of the peptide (Fig. 7), whereas amiloride K_i obtained with the chimera with the γ N terminal was not different from those obtained with wild-type γ .

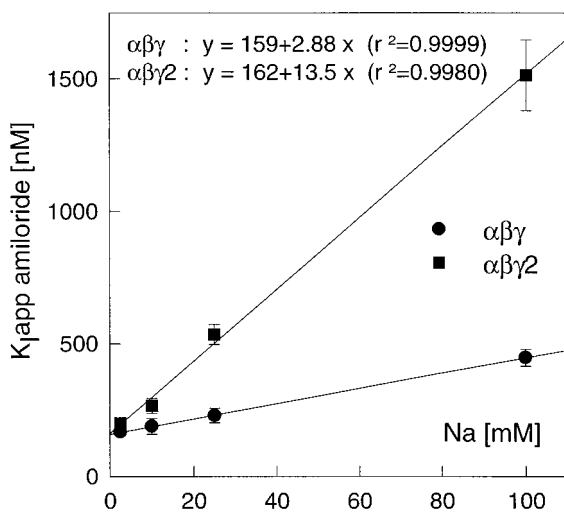


FIG. 6. Na-/amiloride interaction. The graph reports the apparent affinity for amiloride as a function of the extracellular Na^+ concentration. Each point represent a group of 8–14 oocytes in which the response to 5 concentrations of amiloride was measured in a concentration of extracellular Na^+ current. Experiments were performed in parallel on a similar number of oocytes expressing the $\alpha\beta\gamma$ and $\alpha\beta\gamma_2$ isoforms of XENaC. The parameters of the regression lines for the two isoforms are indicated above the graph.

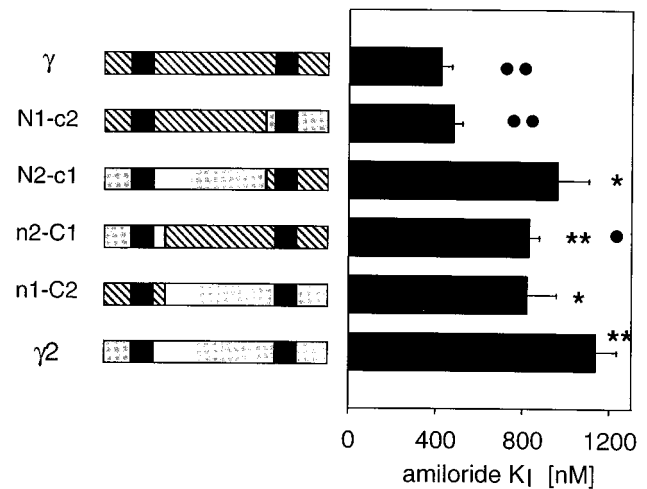


FIG. 7. Amiloride affinity in γ/γ_2 chimeric constructs. The inhibition constant (K_i) for amiloride was measured in oocytes injected with α and β subunit cRNA and either γ , γ_2 , or one of the four chimeric constructs cRNA. The scheme shows the structure of the chimera with the γ part hatched and the γ_2 part shaded. The position of the two hydrophobic segments is indicated by solid boxes. The statistical significance of the differences is indicated as follows: * and ** indicate $P < 0.01$ and $P < 0.001$, respectively, when compared with the γ group. • and •• indicate $P < 0.01$ and $P < 0.001$, respectively, when compared with the γ_2 group.

DISCUSSION

Amiloride-sensitive electrogenic Na^+ transport is carried out by several amphibian epithelia that belong to organs (kidney, lung, skin, colon) with largely different functions. The ionic composition of the external media to which these epithelia are also widely different, suggesting that different forms of the channel might be needed to perform the task of transepithelial Na^+ transport. In amphibian as well and in mammals, the epithelial Na channel appears to be made of three homologous subunits α , β , and γ (8, 14). The indication by Northern blot analysis of amphibian tissues of the possible presence of additional gene products reacting with the probes for the α , β , and γ subunits of XENaC prompted us to investigate the existence of isoforms of these subunits. Our search led to the discovery of two new gene products that, because of sequence similarity, we consider as isoforms of the β and γ subunits and therefore termed β_2 and γ_2 .

X. laevis is a tetraploid organism following a genome duplication that occurred some 30 millions years ago (19). It was therefore reasonable to ask whether the β_2 and γ_2 XENaC genes might have resulted from the genome duplication. In an attempt to answer this question, we compared the degree of identity between β and β_2 XENaC and γ and γ_2 XENaC, respectively, to that of other duplicated genes of *Xenopus*. Using Lipman-Pearson protein alignment we obtained the following percentages of identity: actin (99.7% over 377 codons) and integrin β_1 subunit (97.6% over 798 codons) are well conserved, whereas insulin (92.5% over 106 codons) and albumin (88.8% over 606 codons) are quite divergent for duplicated genes in the same organism. If we compare the values we calculated for β and β_2 (92.7% over 647 codons) and γ and γ_2 (90.0% over 663 codons), it appears that the degree of similarity between these channel subunits is lower than between the average duplicated *X. laevis* proteins, but still falls well within the range of values found for certain duplicated genes like albumin (19). Two hints argue against the duplication being related to tetraploidy: we were never able to identify a second α subunit either by library screening or by looking for a second transcript on Northern blots. In addition, the observation of more than two transcripts for β XENaC suggests the existence of more than two β subunits or at least isoforms resulting from alternative splicing. It was however not possible to decide from these observations if the β/β_2 and γ/γ_2 gene duplications are, or

are not, related to the whole genome duplication. This point is of relatively minor importance since, in any case, the γ_2 protein has acquired biological and physiological properties that are different from the parent γ protein. Differential tissue distribution and expression during development has indeed already been observed for pairs of duplicated proteins in *Xenopus* (19). Whatever the precise time of the gene duplication, and considering the high degree of homologies, it is probable that the divergence between β and β_2 —and, similarly, between γ and γ_2 —has occurred after the divergence of the mammalian and the amphibian lineage. It is therefore difficult to evaluate how much of this finding might be relevant for mammalian species.

The tissue distribution of the new β_2 subunit is qualitatively different from the β isoform; β_2 transcript is more abundant in kidney than in lung relative to the β transcript. There was a large difference in expression of the β_2 and γ_2 transcripts between cells grown on permeable support and cells grown on plastic. It appears therefore that the expression of these genes is regulated according to cell type and the state of differentiation of these cells. The existence of isoforms may have a functional significance, either because of the expression of channel with different physiological characteristics, as those shown for the γ subunit isoforms, or because the expression of isoform can be controlled by different promoters and thus regulated by different signals.

Our initial physiological characterization did not allow us to detect any gross difference in the physiological properties of channels including the β_2 subunit when compared with those containing the β subunit. Because this characterization was rather elementary does not mean that there are no functional differences between these two isoforms. Regarding the γ subunit, there was an obvious difference of affinity for amiloride, with a 3-fold lower affinity for the oocytes expressing the γ_2 isoform (coexpressed either with $\alpha\beta$ or $\alpha\beta_2$) compared with those expressing the γ isoform. In addition, the kinetics of the activation of the Na^+ current through the channel were clearly different: the $\alpha\beta\gamma_2$ isoform had an higher apparent affinity for Na^+ with a current/concentration relationship indicating the presence of more than one binding site, and supporting the presence of an inhibitory binding site for external Na^+ . The physiological relevance of this difference resides in the fact that Na^+ entry into cells expressing this type of channel would be strongly limited at Na^+ concentration higher than 5 or 10 mM. It may allow a large flow of sodium reabsorption at low Na^+ concentrations, while avoiding excessive Na^+ load to the epithelial cell in case of an increase of Na^+ above the millimolar range.

The mechanism of the block of the epithelial Na^+ channel by amiloride and the relationship between the amiloride binding site and Na^+ binding site(s) has been extensively studied in amphibian model tight epithelia (1). Although most studies have reported a competitive type of antagonist binding between Na^+ and amiloride, there were also data supporting other types of antagonism. The availability of two ENaC isoforms with a difference in Na^+ and amiloride apparent affinity prompted us to reevaluate the role of Na^+ ions in amiloride binding. As shown in Fig. 6, in isoforms $\alpha\beta\gamma$ and $\alpha\beta\gamma_2$, our data fit well with the predictions of a competitive binding model. The binding of amiloride seemed to be about 4- to 5-fold more sensitive to the concentration of Na^+ in the $\alpha\beta\gamma_2$ isoform.

The intrinsic affinity of amiloride, i.e., its affinity in the absence of competing Na^+ ions, was very similar, around 160 nM, in both isoforms. This suggests that the amiloride binding site itself is not different in these two subunits. This result is entirely compatible with those of Schild *et al.* (20), who have recently demonstrated that a short segment preceding the putative second transmembrane domain, the \llcorner pre-M2 \lrcorner segment, contains an essential determinant of amiloride affinity, since there is not a single amino acid difference between the γ and γ_2 isoforms in this region. As amiloride-sensitive current can be reconstituted in the oocyte by

expression of the α subunit alone, it was tempting to conclude that the amiloride binding site was constituted exclusively by the α subunit. However, the data presented by Schild *et al.* (20) showed that mutations in the homologous segments of the three subunits α , β , and γ have analogous effects. These data, and our present data, demonstrate that not only the α subunit but also the other subunits are involved, directly or indirectly, in amiloride binding.

Experiments with γ/γ_2 chimera indicate that the difference in apparent amiloride affinity is determined by the N-terminal part of the peptide, which includes the first hydrophobic region and most of the extracellular loop. Since there was no difference in the intrinsic affinity for amiloride between γ and γ_2 , it seems that the difference in the apparent affinity for amiloride between the two isoforms and the chimeric constructs resulted from a modification of a Na^+ binding site, responsible for the Na^+ -amiloride competition. The fact that a difference of similar amplitude was found between γ and γ_2 for the current activation constant by Na^+ (Fig. 5) and for the Na^+ -amiloride competition (Fig. 6) suggests that a single site for Na^+ is involved in the conduction process and in amiloride binding. The results of the experiments with the chimeras indicate that this sodium \llcorner receptor \lrcorner site, which may be one of the elements responsible for the sodium \llcorner self-inhibition \lrcorner phenomenon, is located in the N-terminal two-third of the molecule, most probably in the extracellular loop. Whether this site is an extracellular site exposed to the bulk solution or a site located in the conduction pathway cannot be determined by our data.

In conclusion, we have identified and cloned two novel isoforms of subunits of the epithelial Na^+ channel and shown that the γ_2 isoform confers new properties to the trimeric channel protein. In addition, the steady-state level of the β_2 and γ_2 XENaC mRNA appears to be tissue specific and dependent on culture conditions. Taken together these findings suggest that one or more subunits of the epithelial Na channel might have evolved to modulate the function of this important sodium transport system.

This work was supported by Grant 31-43384.95 from the Swiss Fonds National de la Recherche Scientifique to B.C.R. and Grant RG 464/96 from the International Human Frontier Science Program to J.-D.H.A.M. was supported by a student fellowship from Glaxo (London).

- Garty, H. & Benos, D. J. (1988) *Physiol. Rev.* **68**, 309–372.
- Garty, H. (1994) *FASEB J.* **8**, 522–528.
- Palmer, L. G. (1992) *Annu. Rev. Physiol.* **54**, 51–66.
- Lifton, R. P. (1996) *Science* **272**, 676–680.
- Palmer, L. G. & Frindt, G. (1986) *Proc. Natl. Acad. Sci. USA* **83**, 2767–2770.
- Eaton, D. C. & Hamilton, K. L. (1988) in *The Amiloride-Blockable Sodium Channel of Epithelial Tissue*, ed. Narahashi, T. (Plenum, New York), Vol. 7, pp. 251–282.
- Benos, D. J., Awayda, M. S., Ismailov, I. I. & Johnson, J. P. (1995) *J. Membr. Biol.* **143**, 1–18.
- Canessa, C. M., Schild, L., Buell, G., Thorens, B., Gautschi, Y., Horisberger, J.-D. & Rossier, B. C. (1994) *Nature (London)* **367**, 463–467.
- Canessa, C. M., Horisberger, J.-D. & Rossier, B. C. (1993) *Nature (London)* **361**, 467–470.
- Voilley, N., Lingueglia, E., Champigny, G., Mattéi, M.-G., Waldmann, R., Lazdunski, M. & Barbry, P. (1994) *Proc. Natl. Acad. Sci. USA* **91**, 247–251.
- McDonald, F. J., Snyder, P. M., McCray, P. B., Jr., & Welsh, M. J. (1994) *Am. J. Physiol.* **266**, L728–L734.
- McDonald, F. J., Price, M. P., Snyder, P. M. & Welsh, M. J. (1995) *Am. J. Physiol.* **37**, C1157–C1163.
- Voilley, N., Bassilana, F., Mignon, C., Merscher, S., Mattei, M. G., Carle, G. F., Lazdunski, M. & Barbry, P. (1995) *Genomics* **28**, 560–565.
- Puoti, A., May, A., Canessa, C. M., Horisberger, J.-D., Schild, L. & Rossier, B. C. (1995) *Am. J. Physiol.* **38**, C188–C197.
- Verrey, F., Schaerer, E., Zoerkler, P., Paccolat, M. P., Geering, K., Kraehenbühl, J.-P. & Rossier, B. C. (1987) *J. Cell Biol.* **104**, 1231–1237.
- Palmer, L. G., Corthésy-Theulaz, I., Gaeggeler, H.-P., Kraehenbühl, J.-P. & Rossier, B. (1990) *J. Gen. Physiol.* **96**, 23–46.
- Good, D. W. & Wright, F. S. (1980) *Am. J. Physiol.* **239**, F289–F298.
- Devereux, J., Haerberli, P. & Smithies, O. (1984) *Nucleic Acids Res.* **12**, 387–395.
- Hughes, M. K. & Hughes, A. L. (1993) *Mol. Biol. Evol.* **10**, 1360–1369.
- Schild, L., Schneeberger, E., Gautschi, I. & Firsov, D. (1997) *J. Gen. Physiol.* **109**, 15–26.